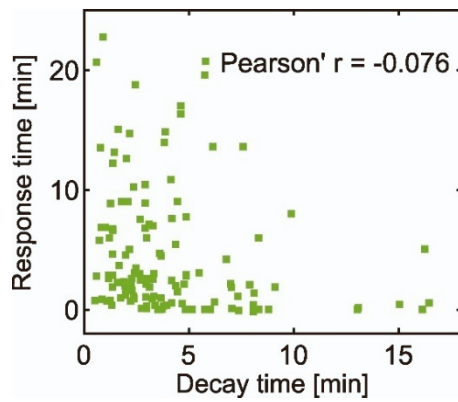


**Cell Reports, Volume 43**

**Supplemental information**

**DNA break induces rapid transcription repression  
mediated by proteasome-dependent RNAPII removal**

**Shuaixin He, Zhiyuan Huang, Yang Liu, Taekjip Ha, and Bin Wu**



**Figure S1.** The decay and response times extracted from fitting TS intensities were not correlated, Related to Figure 1. Scatter data points denoted fits of individual TS intensity traces (n=132 cells). Pearson's correlation coefficient = -0.12, p-value = 0.39.

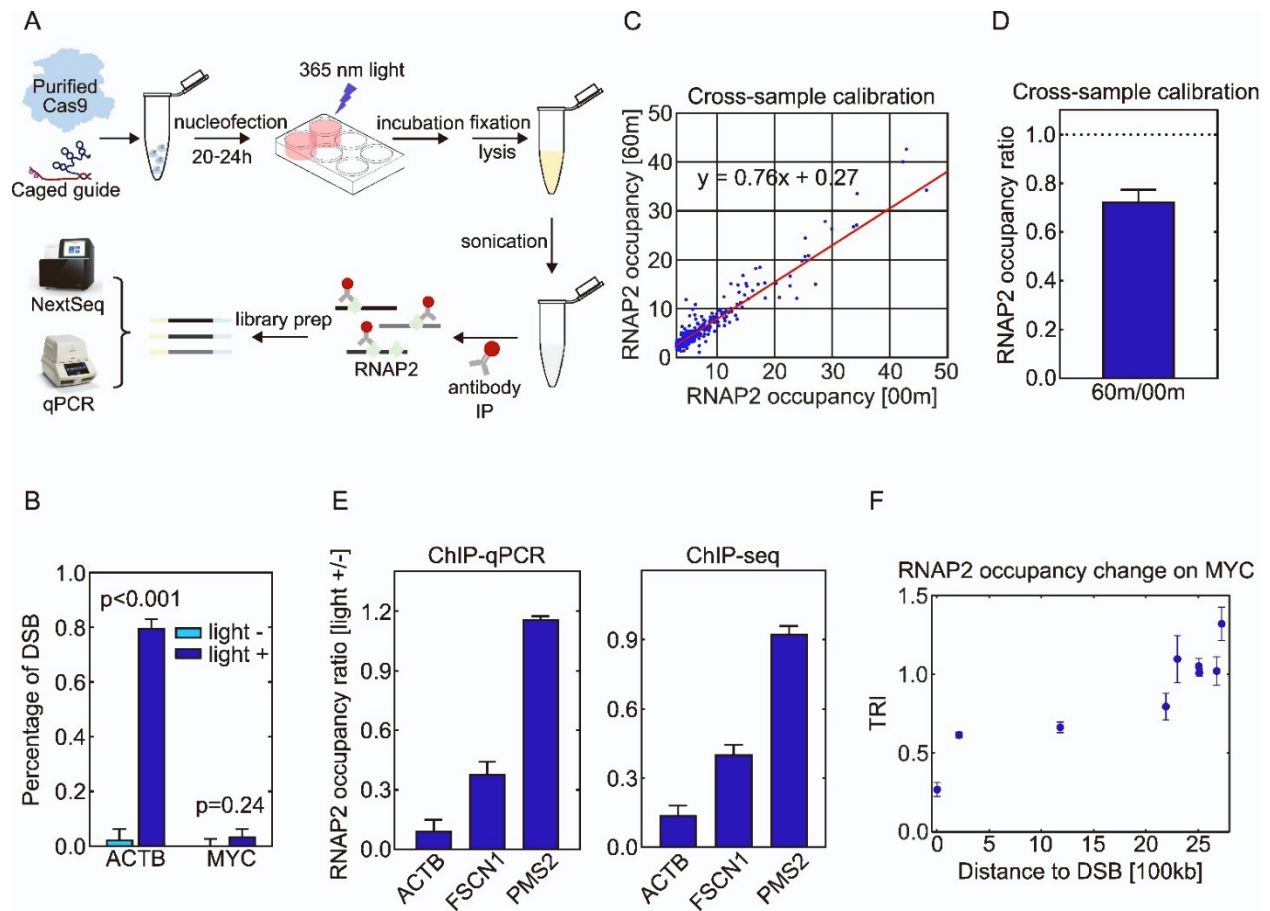


**Figure S2. Change of RNAP2 occupancy after DSB measured by ChIP, Related to Figure 2.**

(A) Schematic of Chromatin Immunoprecipitation (ChIP) with an antibody targeting RNA polymerase II (RNAP2). Purified SpCas9 protein was incubated with caged guide RNA *in vitro* before being electroporated into HEK293T cells. Cells were incubated for 20-24 hours to enable RNP binding. After light stimulation, cells were fixed at certain time points, followed by lysis and sonication. Antibody targeting endogenous RNAP2 was applied for immunoprecipitation (IP). Precipitated genome fragments were further processed to construct libraries, followed by either Illumina sequencing (NextSeq) or qPCR. (B) DSB was efficiently produced on targeted ACTB locus upon light stimulation. Non-targeting MYC locus was a negative control. Cells were fixed at 1 hour after light stimulation and genomic DNA was harvested. DSB was quantified by qPCR

(STAR Methods). Paired student t-test was performed. Error bar: SEM (n=4 biological replicates).

(C) Calibration for RNAP2 occupancy of individual genes between samples. Each sequencing dataset was randomly subset into three technical replicates with 10 million reads. RNAP2 occupancy was calculated for all expressed genes that are not on chromosome 7 (where ACTB is located). The RNAP2 occupancy of individual genes at 0 and 60 minutes after light exposure was shown as a scatter plot (STAR Methods). A linear fitting captured the cross-sample difference. (D) The global RNAP2 occupancy is reduced upon UV exposure. The slope of the fitting in (S2C) was defined as the calibration factor that indicates the difference of RNAP2 occupancy between light-stimulated and no-light samples (STAR Methods) (n=2 biological replicates). (E) Change of RNAP2 occupancy on ACTB locus and nearby genes after light stimulation measured by qPCR (Left) and Illumina sequencing (Right). After library construction, qPCR was performed with the sequencing samples (Amplicons marked in Figure 2A). The measurements of ChIP-seq and ChIP-qPCR are consistent with each other. Error bar: SEM (n=2 biological replicates). (F) Transcription repression propagation from DSB on MYC locus. HEK293T cells were electroporated with Cas9 RNP targeting MYC, fixed at 1 hour after light stimulation and processed for library construction. Illumina sequencing was performed to measure RNAP2 occupancy. Error bar: SEM (n=3 technical replicates).

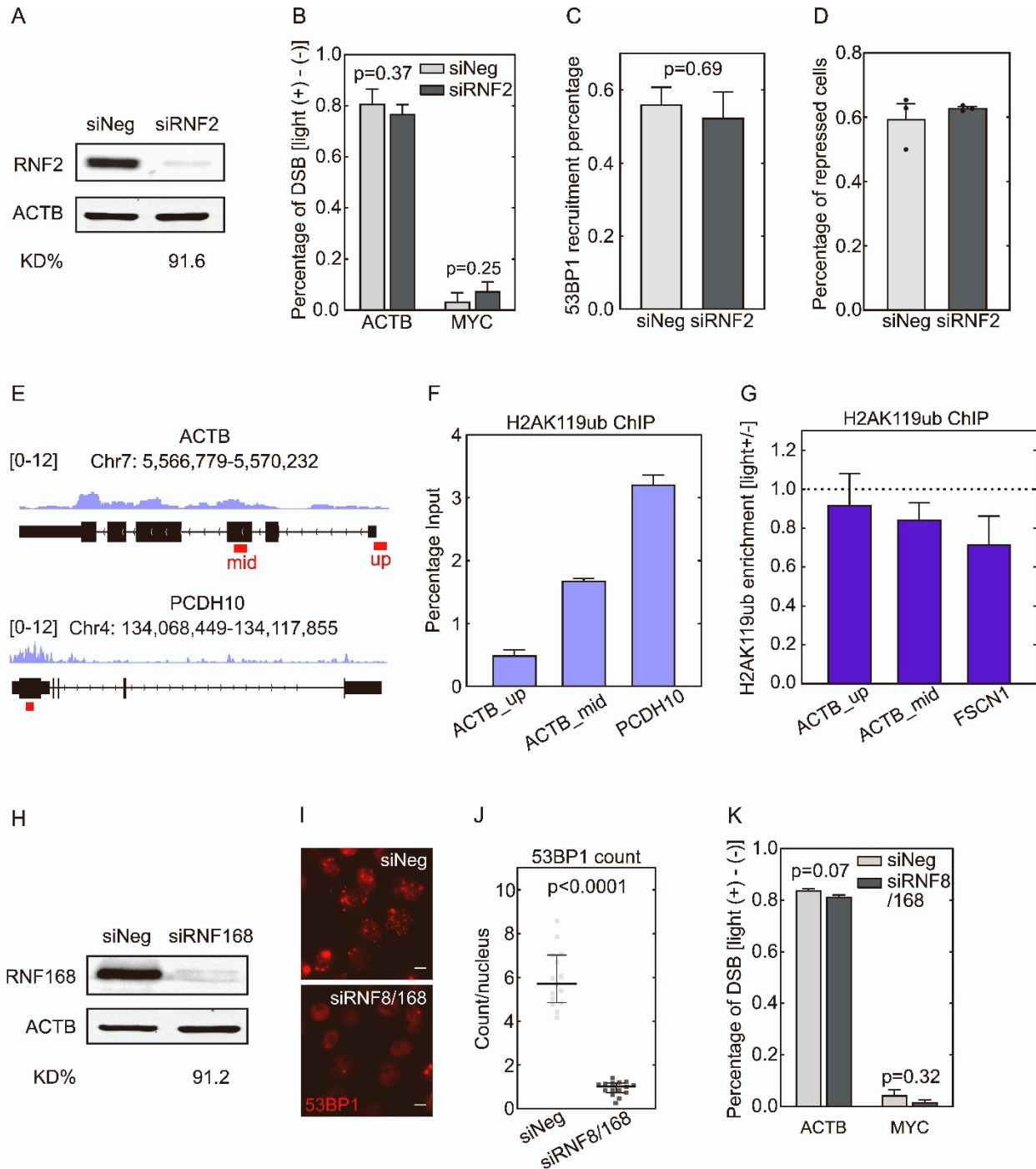


**Figure S3. Perturbing DSB induced transcription repression by siRNA knockdown of RNF2 or RNF8/RNF168, Related to Figure 3.** (A) Knocking down RNF2 with siRNAs. Western Blot showed 91.6% depletion of RNF2 protein after siRNA treatment (siRNF2) compared with negative

control (siNeg). ACTB was used as the internal control. (B) DSB was efficiently produced on targeted ACTB locus upon light stimulation in both RNF2 knockdown samples and negative control. The non-targeting MYC locus showed no DSB. Cells were fixed at 1 hour after light stimulation and genomic DNA was harvested. DSB was quantified by qPCR (STAR Methods). Paired student t-test was performed. Error bar: SEM (n=3 biological replicates). (C) Percentages of cells with 53BP1 recruitment to the DSB site were not influenced by RNF2 knockdown (n=3 biological replicates). Error bar: SEM. An unpaired t-test was performed. (D) Percentages of repressed cells were measured for RNF2 knockdown samples and control samples during 30-minute tracking. All stimulated cells were analyzed. Cells were deemed repressed if the averaged TS intensities in the last 4 frames were lower than a threshold value determined from siNeg control cells with 53BP1 recruitment (Methods) (n=3 biological replicates). (E-G) H2AK119ub was not enriched around DSB. (E) ChIP-qPCR amplicons (red bars) were designed according to the H2AK119ub ChIP-seq dataset (GSM5659337) shown here<sup>1</sup>. PCDH10 locus was used as a positive control for the ChIP experiment. Two amplicons were used to measure H2AK119ub at different regions within ACTB. Error bar: SEM (n=2 biological replicates). (F) The relative enrichment of H2AK119ub at tested sites measured by ChIP-qPCR was consistent with that of the ChIP-seq dataset in (E). (G) H2AK119ub levels at ACTB and FSCN1 did not increase after DSB induction (measured at 60 minutes post light stimulation). Amplicons were denoted by red bars in (E). Error bar: SEM (n=2 biological replicates). (H-J) Knocking down RNF8/168 with siRNAs. (H) Western Blot showed 91.2% depletion of RNF168 protein after siRNA treatment (siRNF8/siRNF168) compared with negative control (siNeg). (I) Representative immunofluorescence images of HEK293T cells showed reduced nuclear 53BP1 foci after siRNF8/siRNF168 treatment compared with siNeg. Scale bar: 5  $\mu$ m. (J) Quantification of nuclear 53BP1 foci number for cells treated with

siRNF8/siRNF168 (n=30 images) and siNeg (n=30 images). Error bar: quartiles. An unpaired Mann-Whitney test was performed. (K) DSB was efficiently produced on targeted ACTB locus upon light stimulation in both RNF8/168 knockdown samples and negative control. The non-targeting MYC locus showed no DSB. Cells were fixed at 1 hour after light stimulation and genomic DNA was harvested. DSB was quantified by qPCR (STAR Methods). Paired student t-test was performed. Error bar: SEM (n=3 biological replicates).

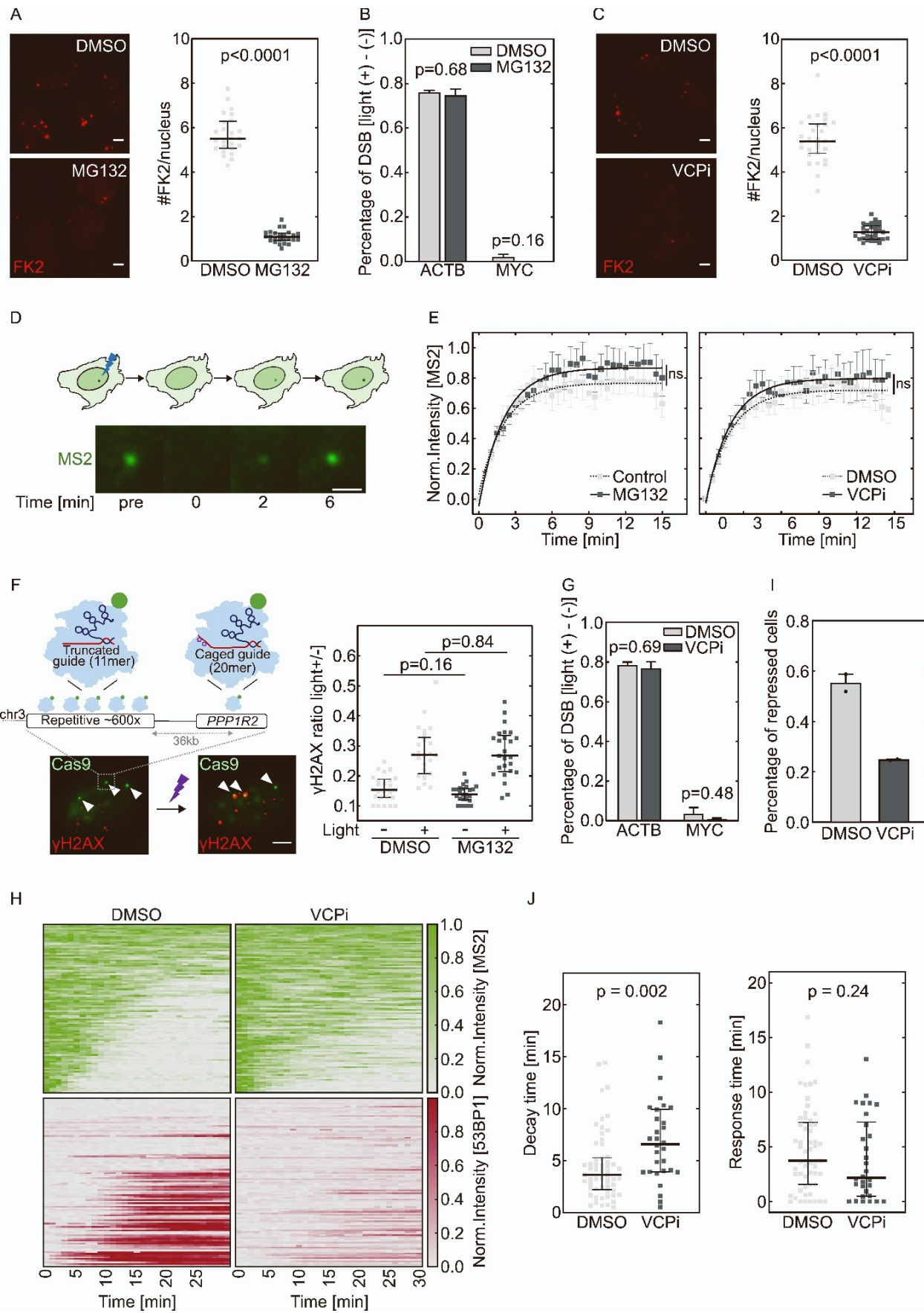




**Figure S4. The effect of proteasome inhibition by MG132 and VCPi on transcription regulation, Related to Figure 4.** (A) Cells were treated with 20  $\mu$ M MG132 for 1 hour to inhibit proteasome. The same amount of DMSO was used as a negative control. Left: representative immunofluorescence images of U-2 OS cells showed reduced nuclear ubiquitination level with FK2 antibody to label conjugated ubiquitin. Scale bar: 5  $\mu$ m. Right: quantification of nuclear FK2 foci number when cells were treated with MG132 (n=30 images) or DMSO (n=30 images). Error bar: quartiles. Mann-Whitney test was performed. (B) DSB was efficiently produced on targeted ACTB locus upon light stimulation in both MG132-treated samples and negative control. The non-targeting MYC locus showed no DSB. Cells were fixed at 1 hour after light stimulation and genomic DNA was harvested. DSB was quantified by qPCR (STAR Methods). Paired student t-test was performed. Error bar: SEM (n=3 biological replicates). (C) Cells were treated with 100  $\mu$ M CB5083 (VCPi) for 1 hour to inhibit VCPATPase. The same amount of DMSO was used as a negative control. Left: representative immunofluorescence images of U-2 OS cells showed reduced nuclear ubiquitination level with FK2 antibody. Scale bar: 5  $\mu$ m. Right: quantification of nuclear FK2 foci number when cells were treated with VCPi (n=30 images) or DMSO (n=30 images). Error bar: quartiles. Mann-Whitney test was performed. (D-E) MG132 and VCPi did not change normal transcription dynamics, measured by FRAP of TS of the live-cell reporter (Figure 1A). (D) Schematic and representative images of FRAP experiment on TS: the TS was photo-bleached with a focused 488 nm laser beam and the signal recovery was tracked for 15 minutes every 30 seconds. Scale bar: 1  $\mu$ m. (E) The recovery of the TS signal did not change significantly when cells were treated with MG132 or VCPi. Cells were treated with 20  $\mu$ M MG132 or 100  $\mu$ M VCPi for 1 hour. Left: MG132, n=18 cells; Control, n=17 cells. Right: VCPi, n=16 cells; Control, n=15 cells. Lines corresponded to fitting with single-exponential association function. Error bar:

SEM. F-test was performed to compare drug treatment and control samples. (F) MG132 did not change the  $\gamma$ H2AX focus signal at the DSB site, indicating no significant perturbation to DSB detection. Cells were treated with 20  $\mu$ M MG132 for 1 hour. Left: experimental scheme and representative immunofluorescence images to measure  $\gamma$ H2AX recruitment to the DSB site. Caged guide RNA targeting the PPP1R2 gene was used for cleavage after light stimulation. Truncated guide RNA targeting the repetitive region near PPP1R2 on chromosome 3 (Chr3Rep) was delivered at the same time to visualize the cleavage site<sup>2</sup>. Colocalization of Chr3Rep (Green) and  $\gamma$ H2AX (Red) denoted DSB generation and detection. Error bar: 5  $\mu$ m. Right: percentage of Chr3Rep loci with colocalized  $\gamma$ H2AX at 1 hour after Cas9 activation (n=30 images for each condition). Error bar: quartiles. An unpaired Mann-Whitney test was performed. (G) DSB was efficiently produced on targeted ACTB locus upon light stimulation in both VCPi-treated samples and negative control. The non-targeting MYC locus showed no DSB. Cells were fixed at 1 hour after light stimulation and genomic DNA was harvested. DSB was quantified by qPCR (STAR Methods). Paired student t-test was performed. Error bar: SEM (n=3 biological replicates). (H-J) DSB-induced transcription repression is regulated by VCP ATPase. Cells electroporated with Cas9 RNP targeting the live-cell transcription reporter (Figure 1A) were treated with 100  $\mu$ M VCPi for 1 hour before imaging. (H) Heatmaps of TS and 53BP1 intensities were measured from live-cell imaging as in Figure 1 (VCPi, n=109 cells; Control, n=100 cells). All stimulated cells were analyzed since there was no 53BP1 recruitment. (I) Percentages of repressed cells were measured for drug treatment and control samples during 30-minute tracking. Cells were considered repressed if the averaged TS intensities in the last 4 frames were lower than a threshold determined in control cells with 53BP1 recruitment. Error bar: SEM (n=2 biological replicates). (J) Transcription decay and response times were obtained by fitting the delayed decay model (Figure 1G) to the repressed

TS intensities in (S4I) (VCPI, n=30 cells; Control, n=57 cells). Error bar: quartiles. An unpaired Mann-Whitney test was performed.

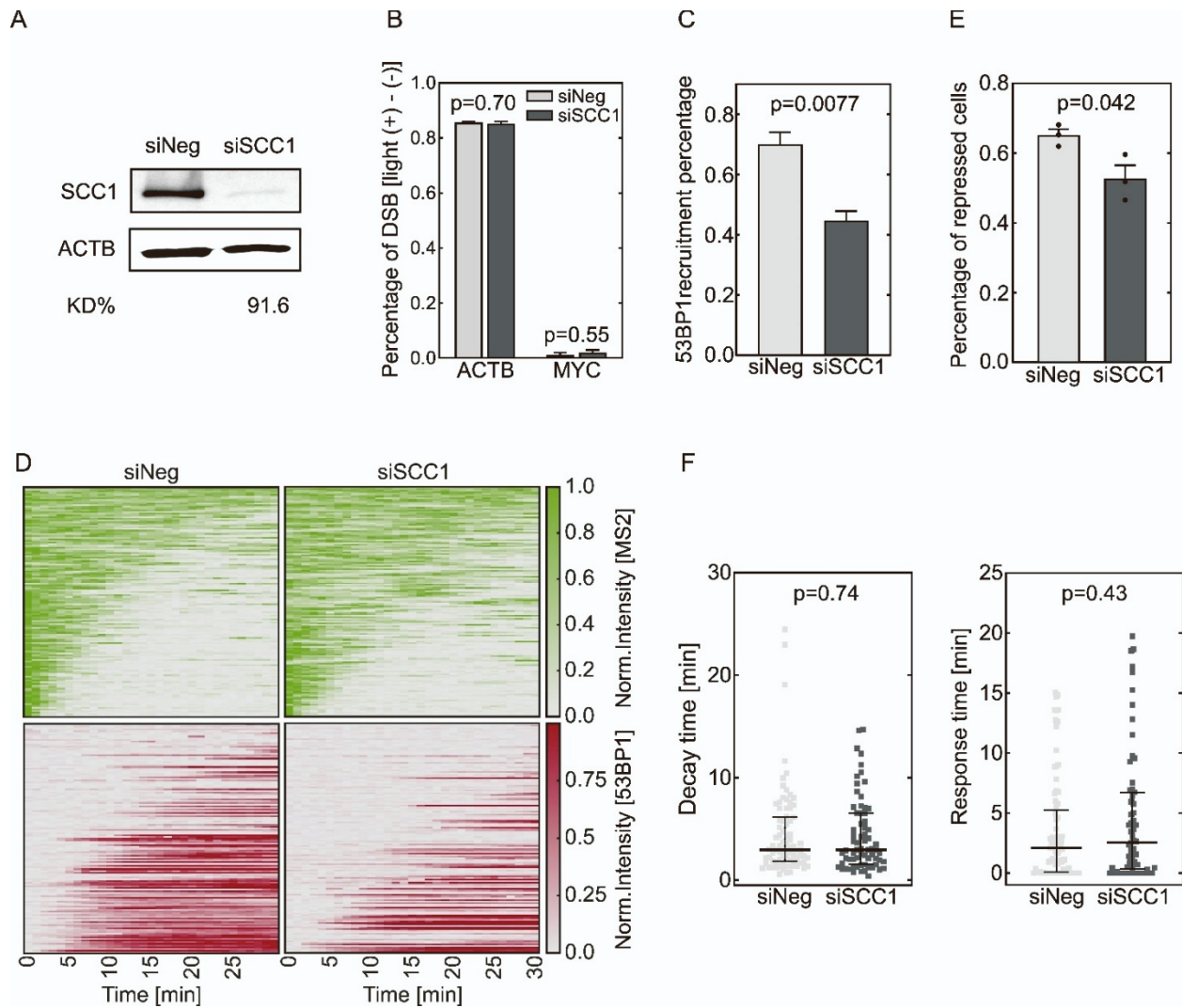


**Figure S5. The influence of cohesin on transcription and 53BP1 recruitment, Related to Figure 5.** (A) Knocking down SCC1 with siRNAs. Left: representative immunofluorescence images of U-2 OS cells showing reduced nuclear SCC1 intensities when treated with siRNA (siSCC1) compared with negative control (siNeg). Scale bar: 5  $\mu$ m. Right: quantification of nuclear SCC1 intensities when treated with siRNA (siSCC1, n=13 images) or control (siNeg, n=20 images). Error bar: quartiles. An unpaired t-test was performed. (A) Knocking down SCC1 with siRNAs. Western Blot showed 91.6% depletion of SCC1 protein after siRNA treatment (siSCC1) compared with negative control (siNeg). ACTB was used as the internal control. (B) DSB was efficiently

produced on targeted ACTB locus upon light stimulation in both SCC1 knockdown samples and negative control. The non-targeting MYC locus showed no DSB. Cells were fixed at 1 hour after light stimulation and genomic DNA was harvested. DSB was quantified by qPCR (STAR Methods). Paired student t-test was performed. Error bar: SEM (n=3 biological replicates). (C) Percentages of cells with 53BP1 recruitment to DSB site for siRNA-treated and negative control (n=3 biological replicates). Error bar: SEM. An unpaired t-test was performed. (D-F) SCC1 showed a minor effect in DSB-induced transcription repression. Cells electroporated with Cas9 RNP targeting the live-cell transcription reporter (Figure 1A) were treated with siRNA targeting SCC1. (D) Heatmaps of TS and 53BP1 intensities were measured from live-cell imaging as in Figure 1 (siSCC1, n=136 cells; siNeg control, n=150 cells). All stimulated cells were analyzed. (E) Percentages of repressed cells were measured for siSCC1-treatment and control samples during 30-minute tracking. Cells were considered repressed if the averaged TS intensities in the last 4 frames were lower than a threshold determined from siNeg control cells with 53BP1 recruitment. Error bar: SEM (n=3 biological replicates). (F) Transcription decay and response times were obtained by fitting the delayed decay model (Figure 1G) to the repressed TS intensities in (S5D) (siSCC1, n=69 cells; siNeg control, n=81 cells). Error bar: quartiles. An unpaired Mann-Whitney test was performed.

<b>Name</b>	<b>crRNA sequences (5' to 3')</b> Green highlights dT-NPOM replacement; Red marks the RNA sequences hybridizing with target DNA
ACTB	GCUAUUCUCGCAGCUCACCA <u>GUUUU</u> AGAGCUAUGCUGUUUUG
MYC	GUAAUCCAGCGAGAGGCAG <u>GUUUU</u> AGAGCUAUGCUGUUUUG
EX2 reporter	CUAUAGUGUCACGGAUCCAG <u>GUUUU</u> AGAGCUAUGCUGUUUUG
<b>Name</b>	<b>tracrRNA sequence (5' to 3')</b>
tracrRNA	AGCAUAGCAAGUAAAAUAAGGCUAGUCCGUUAUCAACUUGAAAAAGU GGCACCGAGUCGGUGCUUU

**Table S1.** Sequences for crRNA and tracrRNA, Related to STAR Methods

Name	Sequences (5' to 3')
DSB_ACTB_F1	TGGCGGCCTAAGGACTCG
DSB_ACTB_R1	GAAGCCGGCCTTGACATG
DSB_ACTB_F2	CACAGGAGCCTCCCGGTTTC
DSB_ACTB_R2	CTTCAGGGTGAGGATGCCTCTC
DSB_MYC_F1	TTGGCGGGAAAAAGAACGG
DSB_MYC_R1	TATTCGCTCCGGATCTCCCT
DSB_MYC_F2	GCCAGCGGTCCGCAAC
DSB_MYC_R2	GAGAGCCTTTCAGAGAAGCGG
ChIP_Pi5_F	AATGATACGGCGACCACCCAGAT
ChIP_Pi7_R	CAAGCAGAAGACGGCATAACGA
ChIP_ACTB_up_F	GCGCCCTATAAAACCCAGC
ChIP_ACTB_up_R	CAAAGGCGAGGCTCTGTG
ChIP_ACTB_mid_F	GGCATCCTCACCCCTGAAGTA
ChIP_ACTB_mid_R	CCACACGCAGCTCATTGTAG
ChIP_ACTB_down_F	GCCCTTCTATGTCTCCCCAG
ChIP_ACTB_down_R	ACTCCCAGGAAATGCAGGTG
ChIP_MYC_F	CATGCCTTGGTTCATCTGGG
ChIP_MYC_R	GGGACACAAATAGAGCTTAGCA
ChIP_GAPDH_F	CCTTCTCCCCATTCCGTCTT
ChIP_GAPDH_R	GAGAAGGGATGGGAGAGAGC
ChIP_FSCN1_F	CAGCCGAACAAAGGAGCAG
ChIP_FSCN1_R	ATGGTGGCAGTAGACGAGAG
ChIP_PMS2_F	AACGTCGAAAGCAGCCAATG
ChIP_PMS2_R	CATGGATGCAACACCCGATC
ChIP_PCDH10_F	GAGAGCCCAGTGTACCAAGT
ChIP_PCDH10_R	CGCGTTGTCATTAGCATCCA

**Table S2.** qPCR primers for DSB detection and RNAP2 ChIP, Related to STAR Methods

Name	Sequences (5' to 3') Red marks the i7 6bp index sequences
MNase_F	/5Phos/GATCGGAAGAGCACACGTCT
MNase_R	ACACTCTTTCCCTACACGACGCTCTTCCGATC*T
PE_i5	AATGATACGGCGACCACCGAGATCTACACTCTTTCCCTACACGACGCTCTTCCGATC*T
PE_i7_01	CAAGCAGAAGACGGCATAACGAGATCGTGATGTGACTGGAGTTCAGACGTGTGCTCTTCCGATC*T
PE_i7_02	CAAGCAGAAGACGGCATAACGAGATACATCGGTGACTGGAGTTCAGACGTGTGCTCTTCCGATC*T
PE_i7_03	CAAGCAGAAGACGGCATAACGAGATGCCTAAGTGACTGGAGTTCAGACGTGTGCTCTTCCGATC*T
PE_i7_04	CAAGCAGAAGACGGCATAACGAGATTGGTCAGTGACTGGAGTTCAGACGTGTGCTCTTCCGATC*T
PE_i7_05	CAAGCAGAAGACGGCATAACGAGATCACTGTGTGACTGGAGTTCAGACGTGTGCTCTTCCGATC*T
PE_i7_06	CAAGCAGAAGACGGCATAACGAGATATTGGCGTGACTGGAGTTCAGACGTGTGCTCTTCCGATC*T
PE_i7_07	CAAGCAGAAGACGGCATAACGAGATGATCTGGTGACTGGAGTTCAGACGTGTGCTCTTCCGATC*T
PE_i7_08	CAAGCAGAAGACGGCATAACGAGATCAAGTGTGACTGGAGTTCAGACGTGTGCTCTTCCGATC*T
PE_i7_09	CAAGCAGAAGACGGCATAACGAGATCTGATCGTGACTGGAGTTCAGACGTGTGCTCTTCCGATC*T
PE_i7_10	CAAGCAGAAGACGGCATAACGAGATAAGCTAGTGACTGGAGTTCAGACGTGTGCTCTTCCGATC*T

**Table S3.** Oligo sequences for ChIP-sequencing library, Related to STAR Methods

### Supplemental References

- [1] Zhou, H., Stein, C.B., Shafiq, T.A., Shipkovenska, G., Kalocsay, M., Paulo, J.A., Zhang, J., Luo, Z., Gygi, S.P., Adelman, K., et al. (2022). Ribosomal RNA degradation contributes to silencing of Polycomb target genes. *Nature* 604, 167–174. 10.1038/s41586-022-04598-0.
- [2] Liu, Y., Zou, R.S., He, S., Nihongaki, Y., Li, X., Razavi, S., Wu, B., and Ha, T. (2020). Very fast CRISPR on demand. *Science* 368, 1265–1269. 10.1126/science.aay8204.